Mode Coupling Effects in Ring-Core Fibres for Space-Division Multiplexing Systems

X.Q. Jin, A. Gomez, Kai Shi, Benn C. Thomsen, Feng Feng, George S. D. Gordon, Timothy D. Wilkinson, Y. Jung, Q. Kang, P. Barua, J. K. Sahu, S. Alam, D. J. Richardson, D.C. O'Brien, and F.P. Payne

Abstract— **An optical fibre with weak mode coupling is desirable for future ultra-high capacity space-division multiplexing (SDM) systems because mode coupling in an optical fibre results in extrinsic loss of the fibre and crosstalk between guided optical modes. To study the feasibility of a ring-core fibre (RCF) for SDM systems, in this paper, we investigate the mode coupling in the RCF supporting 5 or 7 guided mode groups (MGs) at a wavelength of 1550nm. For this purpose, the coupled mode/power theory (CMT/CPT) with identified spatial power spectrum of random perturbations of fibre axis is used to estimate the bend loss/crosstalk of the RCF due to microbending. It is shown that, based on the identified parameters for the spatial power spectrum in the 5/7-MG RCF, the estimated bend loss/crosstalk of the RCF agrees well with experimental results. In addition, the impact of the gradient parameter α and refractive index contrast Δ of the fibre refractive index profile on bend loss and crosstalk of the RCF is explored. Simulation results indicate that the Δ instead of the α significantly affects bend loss and crosstalk of the RCF. The magnitude improvement in bend loss by increasing the Δ is dependent on the spatial power spectrum.**

Index Terms—**Crosstalk, coupled mode/power theory, mode coupling, microbending, ring-core fibre, space-division multiplexing.**

I. INTRODUCTION

To satisfy the ever-increasing bandwidth demand of optical networks in the next decades, space-division multiplexing (SDM) has been considered as a promising technique for future ultra-high capacity optical networks, because it can overcome the capacity bottleneck imposed by the nonlinear Shannon limit in the single-mode fibre (SMF) [1-3]. The SDM aims to provide a sustainable long-term solution for upgrading the optical network capacity in a cost-effective/energy-efficient manner. The application of SDM mainly lies on new transmission optical waveguides which affect energy efficiency and cost saving in capital and operating expenditure. A number of experimental demonstrations have been reported for high-speed spatially multiplexed transmission over the multiple cores or modes in the few-mode/multimode/multi-core/multi-element/ring-core fibres (FMF/MMF/MCF/MEF/RCF) [4-9].

Ring-core fibres (RCFs) have attracted considerable research interest in recent years [9-13] because of its unique advantages: relatively weak mode coupling between high-order azimuthal modes for low-complexity digital signal processing (DSP), large effective area for reducing nonlinear effect, and theoretical prediction of nearly identical gain performance of optical amplifiers. In practice, RCFs are designed to support one radial mode and multiple azimuthal modes for SDM systems. Compared with the traditional MMF which has relatively strong mode coupling among high order optical modes [14], in a RCF, the propagation constant difference between adjacent azimuthal modes significantly increases with increasing azimuthal mode number, which in theory results in relatively weak (strong) mode coupling between high (low) order azimuthal modes. The multiple-input and multiple-output (MIMO) processing used to mitigate the mode coupling effects may be avoided for the signals carried on the high order azimuthal modes experiencing weak mode coupling. The DSP complexity can thereby be reduced by only using MIMO processing to recover signals carried on the low order azimuthal modes and/or optical modes within the same mode group which experience strong mode coupling [13]. A silicon photonic integrated circuit with a circular grating coupler has been demonstrated experimentally [10], which allows an integrated mode conversion into ring shaped modes but further improvement in the insertion loss is required for practical applications. Recent all-fibre photonic lanterns or multi-plane light conversion method exhibit a low insertion loss and good mode selectivity. These techniques can be applied to multiplex a large number of spatial modes in RCFs. In addition, a 6-mode-group ring core multimode erbium doped fiber

X.Q. Jin was with the Department of Engineering Science, University of Oxford, Oxford, OX1 3PJ, U.K. He is currently with the School of Information Science and Technology, University of Science and Technology of China, Hefei, 230026, China. (e-mail: xqjin@ustc.edu.cn)

A. Gomez, D.C. O'Brien, and F.P. Payne are with the Department of Engineering Science, University of Oxford, Oxford, OX1 3PJ, U.K. (e-mail: ariel.gomezdiaz@eng.ox.ac.uk, dominic.obrien@eng.ox.ac.uk, frank.payne@lincoln.ox.ac.uk).

K. Shi and B.C. Thomsen are with the Department of Electronic and Electrical Engineering, University College London, London, WC1E 7JE, U.K. (e-mail: k.shi@ucl.ac.uk, b.thomsen@ee.ucl.ac.uk).

F. Feng, G.S.D. Gordon, and T.D. Wilkinson are with the Department of Engineering, Electrical Engineering Division, University of Cambridge, Cambridge, CB3 0FA, U.K. (e-mail: ff263@cam.ac.uk, gsdg2@cam.ac.uk, tdw13@cam.ac.uk).

Y. Jung, Q. Kang, P. Barua, J. K. Sahu, S. Alam, D. J. Richardson are with the Optoelectronics Research Centre, University of Southampton, Southampton, SO17 1BJ, U.K. (e-mail: ymj@orc.soton.ac.uk, qk1g11@orc.soton.ac.uk, p.barua@soton.ac.uk, jks3@soton.ac.uk, sua@orc.soton.ac.uk, djr@orc.soton.ac.uk).
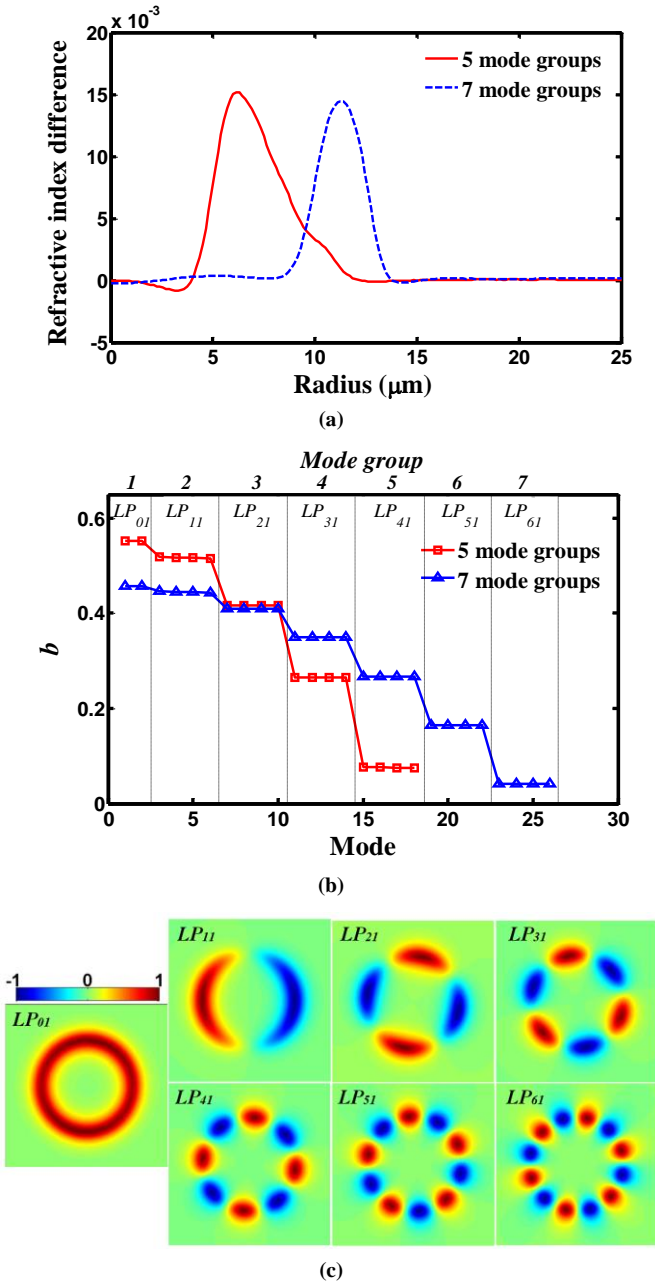
Fig. 1. (a) Refractive index profiles of two fabricated RCFs, (b) its normalized propagation constants b of guided vector modes, and (c) Electric field distributions of LP modes in the 7-MG RCF. Wavelength: 1550nm.

azimuthal and radial mode index, respectively. When $l\geq1$, the LP mode has two-fold spatial degeneracy in each polarization. Figs. 1(a-c) show the measured RIPs of these two fabricated RCFs, normalized propagation constant of vector modes and electric field distributions of corresponding LP modes calculated with the RIPs, respectively. The experimental characterisation of the RCFs shows that the RCF supporting 7 mode groups suffers a large insertion loss of a few hundred dB/km, whilst the RCF supporting 5 mode groups has a relatively low insertion loss of a few dB/km [21-23]. It is noted that those fabricated RCFs supporting a large number of spatial modes or mode groups suffer a large insertion loss [17, 19, 21], which restricts their applications for optical communications. Therefore, it is vital to investigate the cause of such a large insertion loss and impact of key parameters of the RCF design on extrinsic loss of the RCF.

It is well known that microbending plays an important role in the loss of optical fibres because microbending is one of key extrinsic effects increasing attenuation of an optical fibre, apart from the inherent low material loss of optical fibres [24]. Microbending occurs in practice when the bending radius is smaller than 1mm, and causes mode coupling between a guided mode and other guided modes or cladding modes, which results in the crosstalk between optical modes and the extrinsic loss of the fibre. The extrinsic loss arises from the heavily attenuated power of the cladding modes due to the lossy plastic jacket surrounding the optical fibre. The origin of microbending is usually the lateral contact of the optical fibre with rough surfaces and imperfect optical fibre fabrication processing, which result in high-frequency random perturbations of the fibre core along the fibre axis. Given the difficulty in obtaining characteristics of random perturbations in a practical optical fibre, most research on microbending loss was carried out in theory or simulation. Analytical expressions used to predict mode coupling coefficients indicate that the mode coupling between optical modes due to microbending is mainly dependent on the autocorrelation function of the random perturbations and fibre design [24-26].

For a practical RCF, the microbending induced loss and crosstalk may be different from the traditional central core optical fibres, because 1) the special ring-shape RIP of the RCF may result in a special autocorrelation function of the random perturbations of the fibre axis; 2) the RCF has special mode field and normalized propagation constant distributions as seen in Fig. 1. Recently, we presented an analytical model for microbending in optical fibres with arbitrary refractive index profiles due to random perturbations of the fibre core along the fibre axis, and investigated microbending loss of the traditional SMF/MMF and typical RCF/FMF for SDM systems [27]. Numerical results have shown that the RCF and SMF have nearly equal microbending loss of the fundamental mode, which is about two (five) orders of magnitude higher than the FMF (MMF). It is noted that only the fundamental mode is considered for fair comparison between different types of optical fibre in [27].

To further explore the mode coupling effects in RCFs, in this paper, we focus on the investigation of the microbending

amplifier (EDFA) was proposed, which is shown to be capable of providing nearly identical gain among the 6 mode groups within the C band using either a core or cladding-pumped scheme [12].

Both theoretical and experimental investigations have been undertaken for the design of the RCF and modal characteristics in SDM systems [15-21]. Recently, we have designed and fabricated two RCFs with a large refractive index contrast of ~0.01 supporting 5 or 7 mode groups (MGs) (18 or 26 vector modes) at 1550nm for SDM transmission [20-23]. The modes in mode group $(l+1)$ normally correspond to the linearly polarized (LP$_{lm}$) modes ($l\geq0$, $m=1$), where l and m are the

induced bend loss of different guided mode groups and crosstalk in two RCFs supporting 5/7 mode groups, which we recently designed and fabricated [20-23]. With the coupled mode/power theory (CMT/CPT) for the wave propagation analysis [25], the bend loss and crosstalk of the RCFs due to microbending are estimated to fit into the experimental result. Two sets of parameters for the spatial power spectrum in the 5/7-MG RCFs are identified, based on which the impact of key parameters of the RCF design on the bend loss/crosstalk is discussed. These parameters include ring-core radius, gradient parameter α and refractive index contrast Δ of the RCFs.

II. MICROBENDING LOSS AND IMPULSE RESPONSE FROM COUPLED MODE/POWER THEORY

For an optical fibre with microbends, the distorted refractive index profile $n(r, \varphi, z)$ can be written as a first order Taylor series expression [25].

$$n(r,\varphi,z)=n_0(r)+\frac{\partial n_0}{\partial r}f(z)\cos(\varphi) \tag{1}$$

where $n_0(r)$ is the undistorted refractive index profile of a perfect fibre, and r is the radial coordinate of a cylindrical coordinate system. $f(z)$ represents random perturbations of the fibre core along the fibre axis. The loss due to microbending is determined by coefficients of mode coupling between a guided mode and discrete cladding modes. The formula for these coefficients includes an integral in the r, φ-plane over the product $[n(r,\varphi,z)-n_0(r)]E_{lm}E_{l'm'}$. Here, E_{lm} (or $E_{l'm'}$) is the guided (or cladding) mode field, which can be expressed as $A_{lm}(r)\cos(l\varphi)\exp(-j\beta_{lm}z)$ (or $A_{l'm'}(r)\cos(l'\varphi)\exp(-j\beta_{l'm'}z)$). β is the mode propagation constant. Since the refractive index difference $(n-n_0)$ contains a term of $\cos(\varphi)$, the coefficients of the mode coupling in the fibre have nonzero values when the azimuthal mode index difference between the guided and cladding modes $|l-l'|$ is one. Therefore, the microbending loss coefficient of a guided mode can be written as [25]

$$2\gamma_{lm}=\sum_{m'=2}^{\infty}\frac{k_0^{\;2}}{2}\widetilde{R}(\Delta\beta_{lm,l'm'})\frac{\left(\int_0^{\infty}\frac{\partial n_0}{\partial r}A_{lm}A_{l'm'}rdr\right)^2}{\int_0^{\infty}A_{lm}^{\;2}rdr\int_0^{\infty}(A_{l'm'})^2rdr}$$
$$|l-l'|=1 \tag{2}$$

where $k_0=2\pi/\lambda$ is the free-space wavenumber (λ is wavelength in the free space) and $\Delta\beta_{lm,l'm'}$ is the propagation constant difference between guided and cladding modes. $\widetilde{R}(\Delta\beta)$ is the spatial power spectrum of the autocorrelation function of $f(z)$. To represent a wide range of autocorrelation functions, the spatial power spectrum is given by the form [27],

$$\widetilde{R}(\Delta\beta)=\frac{C\sigma^2}{1+(\Delta\beta L_c)^{2p}} \tag{3}$$

$$C=\left[\int_{-\infty}^{\infty}\frac{1}{1+(\Delta\beta L_c)^{2p}}d\Delta\beta\right]^{-1} \tag{4}$$

where L_c is correlation length and σ is the standard deviation of the random perturbation function $f(z)$. A typical value of p is 1, 2, or 3 depending on the external stress on the fibre and fibre

fabrication processing.

In order to obtain the impulse response of the RCF-based transmission link for the analysis of crosstalk, mode coupling in the RCF is modelled with the coupled power theory or following coupled power equation derived by Marcuse [28].

$$\frac{dP_i}{dz}+\tau_i\frac{dP_i}{dt}=-2\gamma_iP_i+\sum_{i'}\Gamma_{ii'}(P_{i'}-P_i) \tag{5}$$

where P_i, τ_i, and γ_i are the power, delay per unit length and power attenuation coefficient of guided mode i, respectively. Assuming that the inherent low loss of the optical fibre is negligible, the mode power attenuation coefficient can be determined by Eq. (2). $\Gamma_{ii'}$ is the mode coupling coefficient between mode i and i', which can be expressed as [26,28]

$$\Gamma_{ii'}=\widetilde{R}(\Delta\beta_{ii'})\cdot|K_{ii'}|^2 \tag{6}$$

$$K_{ii'}=\frac{\pi\omega e_0}{2j}\int_0^{\infty}\frac{\partial n_0}{\partial r}A_iA_{i'}rdr \tag{7}$$

The mode coupling coefficient is calculated with the electric field for each mode normalized as follows.

$$\int_0^{\infty}rA_i^{\;2}dr=\frac{k_0}{\pi\beta_i}\sqrt{\frac{\mu_0}{e_0}} \tag{8}$$

where e_0 and μ_0 are vacuum permittivity and vacuum permeability, respectively. As seen from Eqs. (6-8) that the mode coupling coefficient Γ consists of two parts: the spatial power spectrum $\widetilde{R}(\Delta\beta)$ determined by the environment surrounding the fibre and fibre fabrication processing, and the coefficient K determined by the fibre design (n_0). In the following, discussion is given to the impact of both the spatial power spectrum $\widetilde{R}(\Delta\beta)$ and the fibre design on bend loss/crosstalk of the RCF.

III. SIMULATION CONDITIONS AND PARAMETERS

To study the impact of the fibre design on bend loss/crosstalk of the RCF, the refractive index profile of the RCF is defined as

$$n_0(r)=\begin{cases} n_a\left[1-2\Delta\left(\frac{r-r_a}{d/2}\right)^{\alpha}\right]^{1/2} & |r-r_a|\le d/2 \\ n_a(1-2\Delta)^{1/2} & |r-r_a|>d/2 \end{cases} \tag{9}$$

where n_a is the peak refractive index in the ring-core layer, and Δ is the refractive index contrast. r_a and d are the average radius and thickness of the ring-core layer, respectively. The normalized propagation constant is defined as $b=[(\beta/k_0)^2-n_c^{\;2}]/(n_a^{\;2}-n_c^{\;2})$, where n_c is the cladding index. The measured RIPs in Fig. 1(a) or defined RIP in Eq. (9) are used to obtain the vector mode properties (propagation constants, delay and electric fields) at a wavelength of 1550nm with Comsol.

Since the cladding of the RCF is also an optical waveguide and can be considered as a multimode fibre, it can support a number of cladding modes, which are similar to guided modes. The difference is that the field of a cladding mode is distributed over the whole cladding, and in practice can penetrate through its external boundary between the cladding and coating. As a result, when light travels through a RCF, a cladding mode

gradually loses energy, which is absorbed by the lossy medium in the coating. For simplicity, the perfectly matched layer (PML) is used as the absorbing boundary condition for the cladding without reflection of obique incident waves in Comsol. 500 vector modes including both guided and cladding modes are used for the calculation of the bend loss in Eq. (2), where the real part of the complex propagation constants of the cladding modes is considered.

The crosstalk of the RCF is calculated from the impulse response of the RCF link obtained from Eq. (5). With a split-step method [29], Eq. (5) can be solved numerically when the step Δz is smaller than inverse of maximum value of $\Gamma_{ii'}$. The value of Δz is chosen to be $<(20\Gamma_{max})^{-1}$ for high accuracy of channel modelling here, where Γ_{max} is maximum value of $\Gamma_{ii'}$. In calculating crosstalk between guided optical modes in the RCF, a mode group carrying a single Gaussian pulse is excited at the input of the RCF to obtain the crosstalk between the launched mode group and other mode groups with the received power in each mode group. The impulse response of the RCF link can also be used to verify the bend loss obtained in Eq. (2). The full-width half-maximum (FWHM) of the Gaussian pulse is 36ps, which corresponds to the 28Gbaud quadrature phase shift keying (QPSK) signal adopted for experimental measurement of crosstalk [23]. An ideal low-pass filter is used to simulate the limited electrical bandwidth of 25GHz for the coherent receiver in the experiment.

IV. MICROBENDING LOSS AND CROSSTALK OF THE RCFS

With the mode coupling theory and model of the optical fibre link described in Section II, investigation is made of comparisons in microbending loss/crosstalk between numerical and experimental results. After that, detailed numerical results are given to explore the impact of the fibre design on microbending loss and crosstalk of the RCFs. As each mode in a mode group suffers equal loss due to microbending, for simplicity, guided mode groups instead of vector modes are used for analysis although vector modes or degenerate modes can also be used for mode division multiplexing applications.

A. Comparisons between experimental and numerical results

The mode dependent loss (MDL) was measured by a cutback technique when a guided mode group was selectively launched into the RCFs. A phase-only spatial light modulator (SLM) is used to convert the Gaussian beam from a SMF to a LP mode in a guided mode group in the RCF. By comparing the output power at the end of the 1m and 101m (151m) long 5 (7)-MG RCFs, the loss of the mode group can be obtained. To fit the experimental results with numerical results, a proper spatial power spectrum of the autocorrelation function needs to be identified. It can be seen from Eqs. (2-3) that the σ determines the average microbending loss of the RCF, whilst the correlation length L_c and p determine the slope of the spatial power spectrum or the distribution of the microbending loss on all the mode groups. In practice, the last few guided mode groups usually suffer relatively large loss due to the small propagation constant difference between the guided modes and cladding modes. The trend of increased loss in the last few
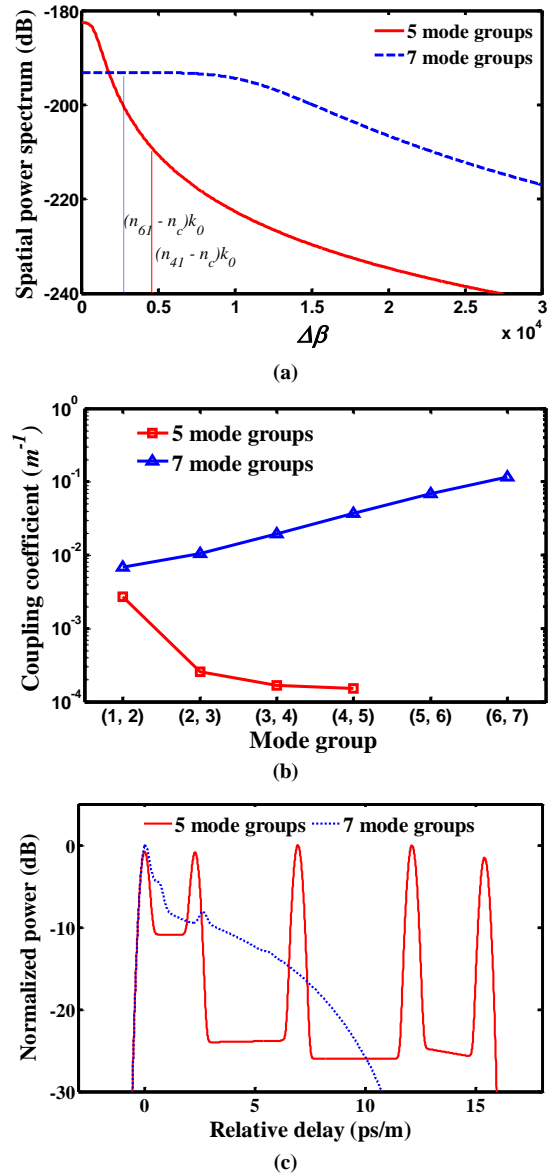

Fig. 2.(a) Spatial power spectrum of the autocorrelation function for the 5/7-MG RCF; (b) Coupling coefficient between two adjacent mode groups, (c) Impulse responses of the 100m 5/7-MG RCFs when all the guided modes are excited at the input with equal power.

guided mode groups together with the mode loss distribution can be used to estimate the values of the L_c and p. With the above knowledge, a set of parameters, $\sigma=35nm$ (35nm), $L_c=1mm$ (0.083mm) and $p=2$ (3), were identified for the 5 (7)-MG RCF. The graphs of the spatial power spectrum and the coupling coefficient between neighbouring mode groups obtained with the identified parameters are given in Fig. 2(a, b). It shows that the spatial power spectrum for the 5-MG RCF is much lower than that for the 7-MG RCF in the range $\Delta\beta > (n_{lg}-n_c)k_0$, where n_{lg} is effective index of the last guided mode group. It implies relatively weak (strong) mode coupling for the 5 (7)-MG RCF. As shown in Fig. 2(b), the mode coupling coefficient between neighbouring mode groups calculated with Eq. (6) for the 5-MG RCF is also lower than that for the 7-MG RCF. For the 5 (7)-MG RCF, the decrease (increase) in mode
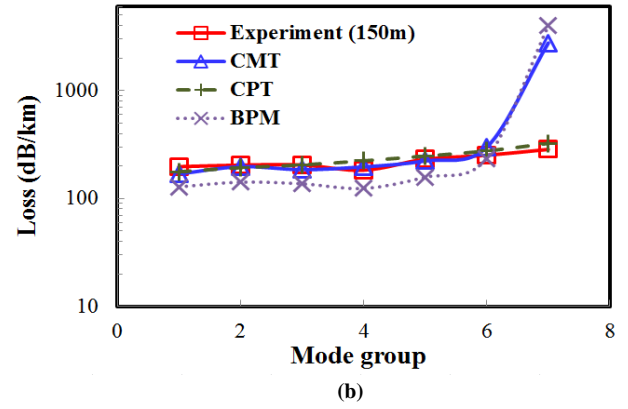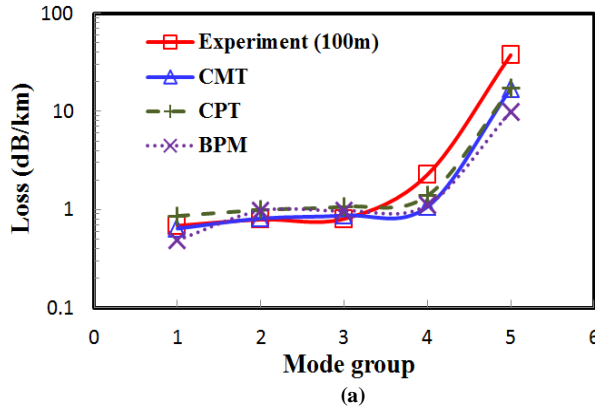
(a)

(b)

Fig. 3. Loss of (a) a 100m 5-MG RCF and (b) 150m 7-MG RCF obtained from experimental measurement and simulation using CMT/CPT/BPM.
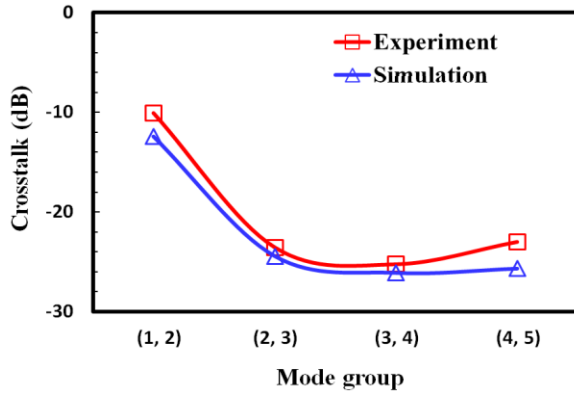

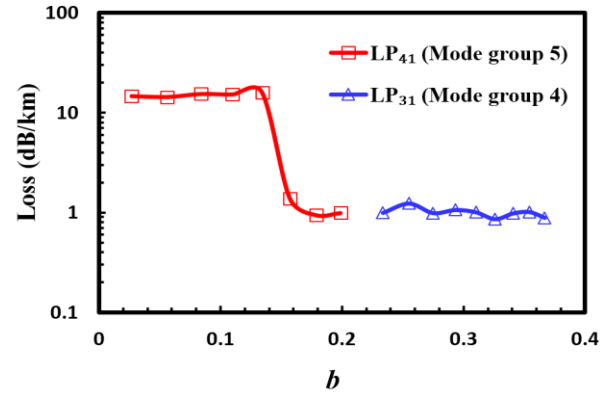Fig. 4. Crosstalk between neighbouring mode groups in the 100m 5-MG RCF.

Fig. 5. Microbending loss of mode group 5/4 (LP_{41}/ LP_{31}) for the 5-MG RCF.

coupling coefficient with increasing mode group index indicates the relatively weak mode coupling in the high (low) order mode groups. This is confirmed from the impulse responses of these two 100m 5/7-MG RCFs in Fig. 2 (c) when all the mode groups are excited with equal power. In the figure, for the 5-MG RCF the plateau between the last two pulses (high order mode groups) due to mode coupling is relatively lower than others between the beginning pulses (low order mode groups). For the 7-MG RCF, the impulse response (mode groups) significantly decreases with increasing relative delay (mode group index) because of the strong mode coupling across all the mode groups and the large coupling coefficient in the high order mode groups as mentioned for Figs. 2(a,b). Therefore, only the first several pulses (low order mode groups) were observed, which is consistent with our experimental observation.

With the identified parameters for the relatively weak (strong) mode coupling in the 5 (7)-MG RCF, the microbending loss of the RCFs is calculated with the CMT/CPT in Fig. 3. As shown in the figure, the graphs of the microbending loss calculated with the CMT for the 5/7-MG RCFs are close to the graphs of the measured MDL, which shows good agreement in microbending loss between simulation and experimental results. To verify the validity of the microbending loss calculated with the CMT, the beam propagation method (BPM) is used to estimate loss of a ~40mm long RCF with microbends [27]. As seen in Fig. 3, the good

agreement in microbending loss between using the CMT and BPM indicates that the analytical expression in Eq. (2) with the form of the spatial power spectrum in Eq. (3) can be used to accurately predict microbending loss of the RCFs. It is interesting to note that, for the 7-MG RCF, the calculated loss of the last guided mode group with the CMT/BPM is higher than the measured loss. This is because the strong mode coupling between the last guided mode group and other guided mode groups or cladding modes in the 7-MG RCF causes the power in the last mode group coupled to the low order mode groups. In this case, the measured MDL has a nearly uniform distribution on all the mode groups. As a consequence, the impulse response of the 7-MG RCF in Fig. 2(c) shows a broad single pulse due to the strong mode coupling. For the 5-MG RCF, the microbending loss given by the CPT also agrees well with the measured loss because of the relatively weak mode coupling between different mode groups.

For the interest of low microbending loss, the crosstalk for the 100m 5-MG RCF is calculated for the comparison with the experimental result in Fig. 4. It shows that the calculated crosstalk between neighbouring mode groups, which decreases with increasing mode group index, agrees well with the experimental values. The measured crosstalk between mode group (4,5) is slightly higher than mode group (3,4) because the last mode group suffers the highest loss due to microbending as shown in Fig. 3(a). The good agreement between the numerical and experimental results confirms again the validity of the
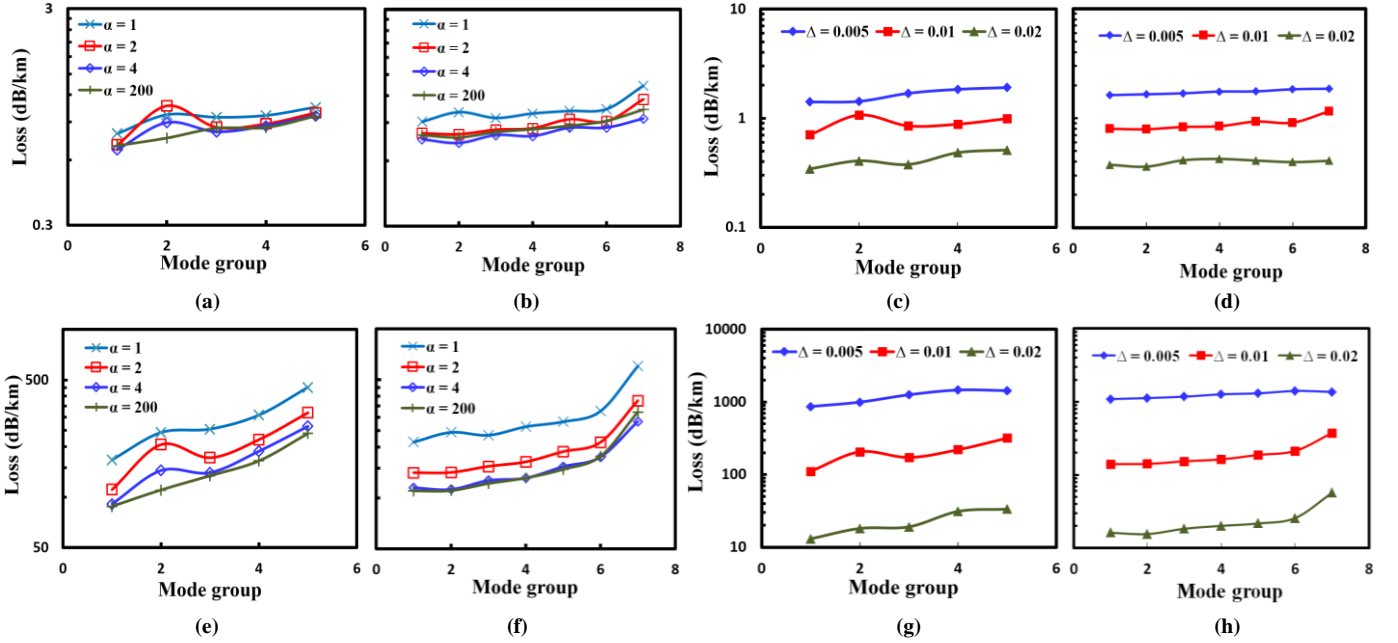
Fig. 6. Microbending loss of the 5/7-MG RCFs for different values of (a,b,e,f) α (Δ =0.01) or (c, d, g, h) Δ (α=2). σ=35nm (a-d): L_c=1mm, p=2; (e-h): L_c=0.083mm, p=3.

identified spatial power spectrum.

B. Impact of fibre design on microbending loss/crosstalk of the RCFs

To explore key parameters of the RCFs affecting SDM applications, in this section, the impact of r_a, α and Δ parameters in the defined refractive index profile in Eq. (9) on microbending loss/crosstalk of the RCFs is investigated with the identified parameters for the relatively weak/strong mode coupling in the 5/7-MG RCFs. In the following simulation, the analytical expression with the spatial power spectrum in Eqs. (2-3) and the coupled power equation in Eq. (5) are used to estimate the microbending loss and crosstalk of the RCFs, respectively.

In practice, the last guided mode group normally suffers the largest microbending loss because its smallest b value among the guided mode groups as seen in Fig. 1(b) means that its effective index is close to the cladding index of the RCFs. An effective way of improving microbending loss of the RCF is to increase the b of the last mode group by varying ring-core radius of the RCFs. As an example, Fig. 5 shows the microbending loss of the last two guided mode groups in a 5-MG RCF, where the parameters Δ=0.01, α=2, d=5.7μm are chosen to mimic the measured RIP in Fig. 1(a). Since the ring-core radius of the RCF affects not only effective index (or b) of azimuthal modes, but also the number of azimuthal modes, in Fig. 5 the ring-core radius varies from 6.0μm to 7.6μm to ensure 5 guided mode groups in the RCF. As shown in the figure, for $b > 0.15$ the microbending loss of the last guided mode group (LP$_{41}$) sharply drops to a minimum value, which is nearly equal to the loss of the last second mode group (LP$_{31}$). Compared with the experimental result in Fig. 3(a), the loss of the last mode group is significantly improved using the optimized ring-core radius, r_a =7.2~7.6 μm (b = 0.15~0.2). To

achieve low microbending loss of the RCFs, in the following simulations, the ring-core radius, r_a, and thickness, d, are set to ensure that the b of the last guided mode group reaches its maximum value, which indicates that the highest effective index of the cladding modes is approximately equal to the cladding index.

After the discussion about the influence of the ring-core radius on the microbending loss of the last mode group, the impact of the refractive index contrast Δ and the gradient parameter α on microbending loss of the 5/7-MG RCFs is presented in Fig. 6. As shown in Figs. 6(a,b,e,f) when Δ=0.01, for the α values from 1 to 200, the overall loss on the mode groups for either 5-MG or 7-MG RCF remains roughly the same, and the microbending loss slightly increases with increasing mode group index. This indicates that the gradient parameter α has a little influence on microbending loss of the RCFs with weak/strong mode coupling. For α=200, the RCFs can be considered to have a step-index profile.

Figs. 6 (c,d,g,h) show microbending loss of the 5/7-MG RCFs for the Δ values of 0.005, 0.01, 0.02 when α=2. The RCFs with a larger Δ have the smallest loss. With the parameters for weak (strong) mode coupling, the loss for the RCFs is improved by two (ten) times when the Δ value is doubled. Such big improvement in microbending loss by a large Δ is due to increased $\Delta\beta$ between neighbouring mode groups. The same magnitude improvement in microbending loss for both the 5/7-MG RCFs indicates that the loss improvement by increasing the Δ is dependent on the spatial power spectrum instead of the number of guided mode groups in the RCFs.

With the calculated microbending loss of mode groups in Fig. 6, the crosstalk between neighbouring mode groups in the 1km 5/7-MG RCFs for different α or Δ values is obtained in Figs. 7(a,b) where the parameters for weak mode coupling are

(a)

(b)

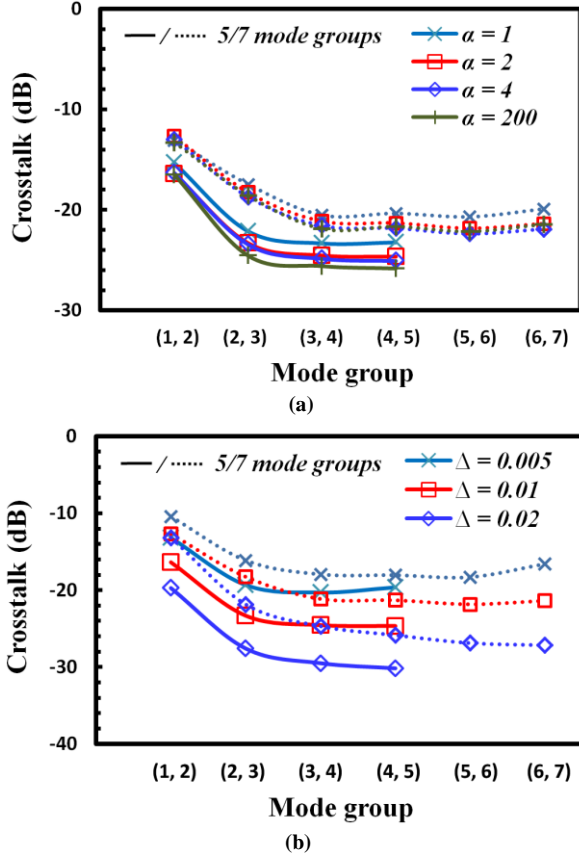Fig. 7. Crosstalk between neighbouring mode groups in the 1km 5/7-MG RCFs for different values of (a) α ($\Delta = 0.01$) and (b) Δ ($\alpha=2$).

Fig. 8. Average crosstalk/microbending loss as a function of number of mode groups.

used. As shown in the figures, the crosstalk for the 5/7-MG RCFs decreases with increasing mode group index, and the 5-MG RCFs always have a crosstalk lower than the 7-MG RCFs for the same α and Δ values. In Fig. 7(a) where $\Delta=0.01$, for the 5/ 7-MG RCFs, the graphs of the crosstalk for different α values are close to each other. It indicates that the α does not significantly affect the crosstalk because the variation of α does not affect propagation constant difference between adjacent azimuthal modes [20]. However, Fig. 7(b) shows a significant improvement in crosstalk by increasing the Δ for the 5/7-MG RCFs. The crosstalk in the high order mode groups is improved more than that in the low order mode groups. To gain a better understanding of the result in Fig. 7(b), Fig. 8 shows the average crosstalk/microbending loss of the RCFs supporting up to 9 (guided) mode groups. As seen in Fig. 8, the increase in Δ results in performance improvement in both crosstalk and microbending loss. The average crosstalk almost linearly increases with increasing the number of (guided) mode groups on a logarithmic scale. This can be explained by the fact that the mode coupling mainly depends on the $\Delta\beta$ between neighbouring mode groups that decreases for an increased number of mode groups. The unvarying average loss for a given value of Δ is because the radial component $A_{lm}(r)$ of guided mode fields affecting the loss in Eq. (2) is mainly determined by the ring-core thickness, which remains at nearly the same
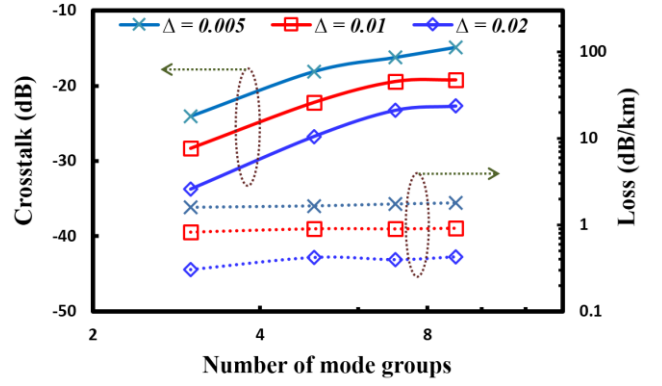
value for different number of mode groups. It also indicates that the cladding modes of the RCFs supporting different number of mode groups are similar to each other. The observed three parallel curves of microbending loss agrees with the result in Fig. 6(c,d). This confirms again that the loss improvement by increasing the Δ is independent of the number of mode groups.

V. CONCLUSIONS

Investigations of the mode coupling effects in the fabricated 5/7-MG RCF have been undertaken using the coupled mode/power theory with the spatial power spectrum of random perturbations of fibre axis, which was identified with the measured MDL. Simulations have shown a good agreement in the microbending induced loss and crosstalk between numerical and experimental results in the 5/7-MG RCF. The impact of the α and Δ parameters of the RCF on microbending loss and crosstalk have also been investigated, which shows that the Δ instead of the α significantly affects the loss and crosstalk of the RCF. The magnitude improvement in microbending loss by increasing the Δ is dependent on the spatial power spectrum. In addition, both experimental and numerical results have shown that RCFs have relatively low crosstalk between high order mode groups, which is different from the traditional MMF or FMF. Such feature indicates the great potential of high-speed data transmission on these high order mode groups in the RCFs.

References

[1] H.R. Stuart,"Dispersive Multiplexing in Multimode Optical Fiber," Science, vol. 289, no. 5477, pp. 281-283, Jul. 2000.

[2] D.J. Richardson, J.M. Fini and L.E. Nelson, "Space-division multiplexing in optical fibres," Nat. Photonics, vol. 7, pp. 354–362, May 2013

[3] P.J. Winzer, 'Scaling optical fiber networks: challenges and solutions,' Optics & Photon. News, Mar. 2015

[4] R. Ryf, S. Randel, A. H. Gnauck, C. Bolle, A. Sierra, S. Mumtaz, M. Esmaeelpour, E. C. Burrows, R.-J. Essiambre, P.J. Winzer, D.W. Peckham, A. H. McCurdy, and R. Lingle, "Mode-Division Multiplexing Over 96 km of Few-Mode Fiber Using Coherent 6 × 6 MIMO Processing", J. Lightwave Technol., vol. 30, no.4, pp. 521–531, Feb. 2012.

[5] Y. Chen, A. Lobato, Y. Jung, H. Chen, V.A.J.M. Sleiffer, M. Kuschnerov, N.K. Fontaine, R. Ryf, D.J. Richardson, B. Lankl, and N. Hanik, "41.6 Tb/s C-band SDM OFDM Transmission through 12 Spatial and

Polarization Modes over 74.17 km Few Mode Fiber," J. Lightwave Technol., vol. 33, no. 7, pp. 1440–1444, Apr. 2015

[6] B.C. Thomsen, "MIMO enabled 40 Gb/s transmission using mode division multiplexing in multimode fiber", Optical Fiber Communication Conference and Exhibition (OFC), (USA, 2010), Paper OThM6

[7] M. Yoshida, S. Beppu, K. Kasai, T. Hirooka and M. Nakazawa, "1024 QAM, 7-core (60 Gbit/s x 7) fiber transmission over 55 km with an aggregate potential spectral efficiency of 109 bit/s/Hz," J. Lightwave Technol., vol. 23, no. 16, pp. 20760–20766, Jul. 2015

[8] S. Jain, V.J.F. Rancaño, T.C. May-Smith, P. Petropoulos, J.K. Sahu, and D.J. Richardson, "Multi-Element Fiber Technology for Space-Division Multiplexing Applications," Opt. Express, vol. 22, no. 4, pp. 3787–3796, Feb. 2014.

[9] N. Bozinovic, Y. Yue, Y. Ren, M. Tur, P. Kristensen, H. Huang, A.E. Willner, and S. Ramachandran, "Terabit-Scale Orbital Angular Momentum Mode Division Multiplexing in Fibers", Science, vol. 340, no. 6140, pp. 1545-1548, Jun. 2013.

[10] C.R. Doerr, N.K. Fontaine, M. Hirano, T. Sasaki, L.L. Buhl, and P.J. Winzer, "Silicon photonic integrated circuit for coupling to a ring-core multimode fiber for space-division multiplexing", European Conference and Exhibition on Optical Communication (ECOC 2011), Paper Th.13.A.3

[11] M. Hirano, Y. Yamamoto, Y. Tamura, T.Haruna and T. Sasaki, "Aeff-enlarged Pure-Silica-Core Fiber having Ring-Core Profile", Optical Fiber Communication Conference and Exhibition (OFC), (USA, 2012), Paper OTh4I.2

[12] Q. Kang, E. Lim, Y. Jun, X.Q. Jin, F.P. Payne, S. Alam, and D.J. Richardson, "Gain Equalization of a Six-Mode-Group Ring Core Multimode EDFA", European Conference and Exhibition on Optical Communication (ECOC 2014), Paper P.1.14

[13] X.Q. Jin, R. Li, D.C. O'Brien, and F.P. Payne, "Linearly Polarized Mode Division Multiplexed Transmission over Ring-Index Multimode Fibres", IEEE Summer Topicals, (USA, 2013), pp. 113-114.

[14] K. Balemarthy, A. Polley, and S.E. Ralph, "Electronic Equalization of Multikilometer 10-Gb/s Multimode Fiber Links: Mode-Coupling Effects", J. Lightwave Technol., vol.24, no.12, pp. 4885-4894, Dec. 2006.

[15] N.K. Fontaine, R. Ryf, M. Hirano, T. Sasaki, "Experimental Investigation of Crosstalk Accumulation in a Ring-Core Fiber", IEEE Summer Topicals, (USA, 2013), Paper TuC4.2

[16] C. Brunet, B. Ung, P.-A. Belanger, Y. Messaddeq, S. LaRochelle, and L.A. Rusch, "Vector Mode Analysis of Ring-Core Fibers: Design Tools for Spatial Division Multiplexing," J. Lightwave Technol., vol. 32, no. 23, pp. 4648–4659, 2014.

[17] C. Brunet, P. Vaity, Y. Messaddeq, S. LaRochelle, and L.A.Rusch, "Design, fabrication and validation of an OAM fiber supporting 36 states," Opt. Express, vol. 22, no. 21, pp. 26117–26127, Oct. 2014.

[18] M. Kasahara, K. Saitoh, T. Sakamoto, N. Hanzawa, T. Matsui, K. Tsujikawa, and F. Yamamoto, "Design of Three-Spatial-Mode Ring-Core Fiber," J. Lightwave Technol., vol. 32, no. 7, pp. 1337–1343, Apr. 2014.

[19] B. Ung, P. Vaity, L. Wang, Y. Messaddeq, L.A. Rusch, and S. LaRochelle, "Few-mode fiber with inverse-parabolic graded-index profile for transmission of OAM-carrying modes," Opt. Express, vol. 22, no. 15, pp. 18044–18055, Jul. 2014.

[20] X.Q. Jin, A. Gomez, D.C. O'Brien, and F.P. Payne, "Influence of Refractive index profile of ring-core fibres for space division multiplexing systems", IEEE Summer Topicals, (USA, 2014), pp.178-179, Jul. 2014

[21] F. Feng, G. S. D. Gordon, X. Q. Jin, D. C. O'Brien, F. P. Payne, Y. Jung, Q. Kang, J. K. Sahu, S. U. Alam, D. J. Richardson, and T. D. Wilkinson, "Experimental characterization of a graded-index ring-core fiber supporting 7 LP mode groups," Optical Fiber Communication Conference and Exhibition (OFC), (USA, 2015), Paper Tu2D.3

[22] F. Feng, X. Guo, G. S. D. Gordon, X. Q. Jin, F. P. Payne, Y. Jung, Q. Kang, S. Alam, P. Barua, J. K. Sahu, D. J. Richardson, I.H. White and T. D. Wilkinson, "All-optical Mode-Group Division Multiplexing Over a Graded-Index Ring-Core Fiber with Single Radial Mode," Optical Fiber Communication Conference and Exhibition (OFC), (USA, 2016), Paper W3D.5..

[23] K. Shi, A. Gomez, X.Q. Jin, Y. Jung, C. Quintana, D.C. O'Brien, F.P. Payne, P. Barua, J. Sahu, Q. Kang, S-U Alam, D.J. Richardson and B.C. Thomsen, "Simplified Impulse Response Characterization for Mode Division Multiplexed Systems," Optical Fiber Communication Conference and Exhibition (OFC), (USA, 2016), Paper W4F.3.

[24] D. Marcuse, "Microbending Losses of Single-Mode, Step-Index and Multimode, Parabolic-Index fibers," Bell Syst. Tech. J., vol. 55, no. 7, pp. 937–955, Sep. 1976.

[25] D. Marcuse, "Microdeformation losses of single-mode fibers.," Appl. Opt., vol. 23, no. 7, pp. 1082-1091, Apr. 1984.

[26] R. Olshansky, "Mode Coupling Effects in Graded-index Optical Fibers", Applied Optics, vol. 14, no. 4, pp. 935-945, April 1975

[27] X.Q. Jin and F.P. Payne, "Numerical investigation of microbending loss in optical fibres", J. Lightwave Technol., vol.34, no.4, pp.1247-1253, Feb. 2016

[28] D. Marcuse, "Derivation of coupled power equations", Bell Syst. Tech. J., vol. 51, no. 1, pp. 229-237, Jan. 1972

[29] D. Yevick and B.Stoltz, "Effect of mode coupling on the total pulse response of perturbed optical fibers", Applied Optics, vol. 22, no. 7, pp. 1010-1015, Apr.1983